Bitlis Eren Üniversitesi Fen Bilimleri Dergisi
BİTLİS EREN UNIVERSITY JOURNAL OF SCIENCE
ISSN: 2147-3129/e-ISSN: 2147-3188
VOLUME: 13 NO: 3 PAGE: 860-870 YEAR: 2024
DOI:10.17798/bitlisfen.1516713

A Machine Learning Prediction Model for Myelitis and Multiple Sclerosis Based on Fourier Transform Features from MRI Images

Züleyha YILMAZ ACAR[1*]

[1]*Selçuk University, Department of Computer Engineering, Faculty of Technology, Konya, Türkiye (ORCID: 0000-0002-4488-478X)*

Keywords: Disease detection, Fast Fourier transform, Machine learning, Myelitis, Neurodegenerative, Statistical features.

Abstract

Myelitis is a neurodegenerative disease positioned in the spinal cord, with multiple sclerosis (MS) being a common subtype. Radiological indicators enable the diagnosis of these diseases. This study proposes a classification framework to detect myelitis, MS, and healthy control (HC) groups using magnetic resonance imaging (MRI) images. The feature extraction step involves applying the fast Fourier transform (FFT) to MRI images. FFT is important because it converts spatial data into the frequency domain, making it easier to identify patterns and abnormalities that indicate these diseases. Then, statistical features (mean, minimum, maximum, standard deviation, skewness, kurtosis, and total energy) are extracted from this frequency information. These features are then used to train support vector machine (SVM), k-nearest neighbor (KNN), and decision tree algorithms. In multi-class classification (myelitis vs. MS vs. HC), the proposed method achieves a classification accuracy of 99.31% with SVM, with average precision, recall, and F1-score values of 99.27%, 99.21%, and 99.24%, respectively, indicating effective classification across all classes. In the binary class classification (HC vs. MS, MS vs. myelitis, HC vs. myelitis), the SVM achieves an outstanding classification accuracy of 99.36%, 99.71%, and 100% respectively. This study highlights the efficiency of FFT-based feature extraction in forming detection patterns for classifying HC, MS, and myelitis classes.

1. Introduction

Myelitis is a neurodegenerative disorder caused by inflammation of the myelin sheath surrounding the nerves in the spinal cord. The disease can cause motor symptoms, sensory symptoms, and autonomic involvement [1]. Various presentations are depending on the site of inflammation [2], [3]. Since multiple sclerosis (MS) is in the common myelitis subgroup, it is important to distinguish between myelitis-non-MS and MS in the diagnosis of the disease. In some cases, it has been observed that myelitis has been observed to be the first sign of MS and may progress to MS [4]. Radiological differentials are known to be more useful in diagnosing the disease [3]. Automatic analysis of radiological images obtained by magnetic resonance imaging (MRI) based on artificial intelligence helps experts in useful aspects such as shortening the diagnosis time and early diagnosis of the disease.

Looking at the studies on automatic diagnosis based on artificial intelligence in the context of neurological diseases, we can see that a wide range of topics have been addressed from the past to the present. Some studies use spatial features extracted by applying wavelet transform to MRI images [5]-[8]. The histogram of oriented gradients (HOG) method has been used to discriminate different structures based on texture shape or gradient change representations in images [9]-[11]. Transfer learning, a type of deep learning, has been used for both feature extraction and classification of raw data in some studies [12]-[15]. In addition to these, there are studies on neurological disease diagnosis by using

*Corresponding author: zuleyhayilmaz@selcuk.edu.tr
Received: 15.07.2024, Accepted: 13.08.2024

various models of deep learning models as classifiers [16]-[19]. Finally, studies using deep learning models as a feature extraction method followed by traditional machine learning algorithms as classifiers are also common [20]-[22].

This paper presents a classification framework for the detection of myelitis, MS, and healthy control (HC) classes. For the first step of feature extraction, which is the most important pre-step of classification, it is proposed to apply the fast Fourier transform (FFT) to the MRI dataset and extract statistical features from the frequency spectrum. The Fourier transform provides frequency information about the signal to which it is applied, allowing the analysis of the image in frequency domain. Then, the machine learning algorithms are fed by the feature set created by extracting statistical features (mean value, minimum value, maximum value, standard deviation, skewness, kurtosis, and total energy) from the resulting two-dimensional FFT output. Support vector machine (SVM), k-nearest neighbor (KNN), and decision tree algorithms are used as classifiers in the study. Multi-class classification based on three classes (HC vs. MS vs. myelitis) and binary class classification (MS vs. myelitis, HC vs. MS, HC vs. myelitis) are evaluated and analyzed. Since, to the author's knowledge, no study has applied a fast Fourier transform to MRI images in this manner. Therefore, this study makes a significant and valuable contribution to the literature, demonstrating high classification success using FFT.

2. Material and Method

The classification framework for myelitis, MS and healthy control groups proposed in the study is depicted in Figure 1. Detailed information about the stages is presented following sections.

2.1. Dataset

A public dataset downloaded from the Kaggle website is used in the study [20]. The myelitis dataset consists of a total of 2,746 spinal MRI images categorized into myelitis-non-MS patients, MS patients, and a healthy control group. Detailed information about the dataset is provided in Table 1.

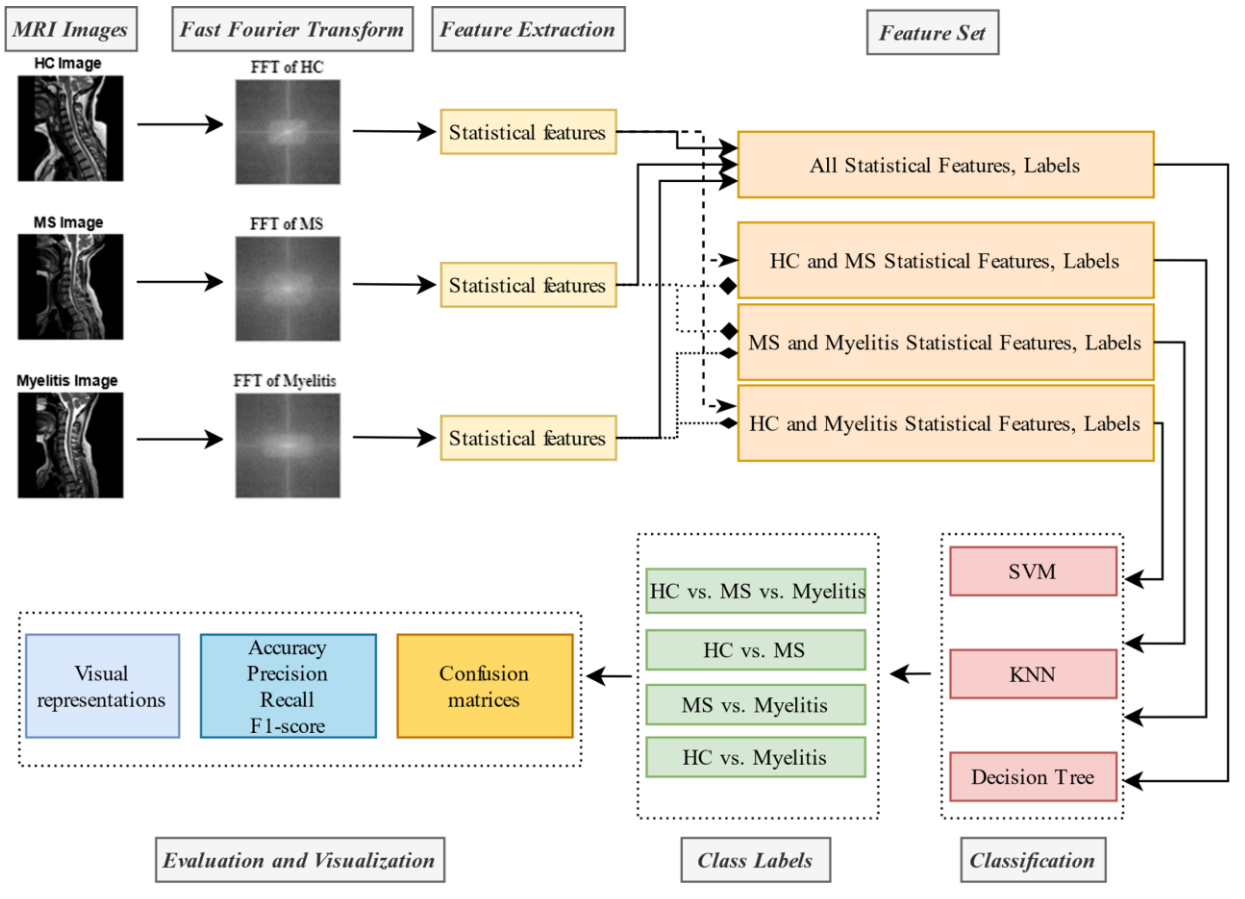

Figure 1. Proposed process of the paper.

Table 1. Details about dataset

Class	Number of images	The class percentages
Myelitis	706	25.71%
MS	667	24.29%
Healthy Control	1,373	50%
Total	2,746	100%

The dataset consists of spinal MRI images. To differentiate between HC, MS, and myelitis classes, the presence of spinal lesions and, if present, vertebral lengths are analyzed. Therefore, spinal MRI images are used in both sagittal and axial planes. Sample images from the dataset are shown in Figure 2.

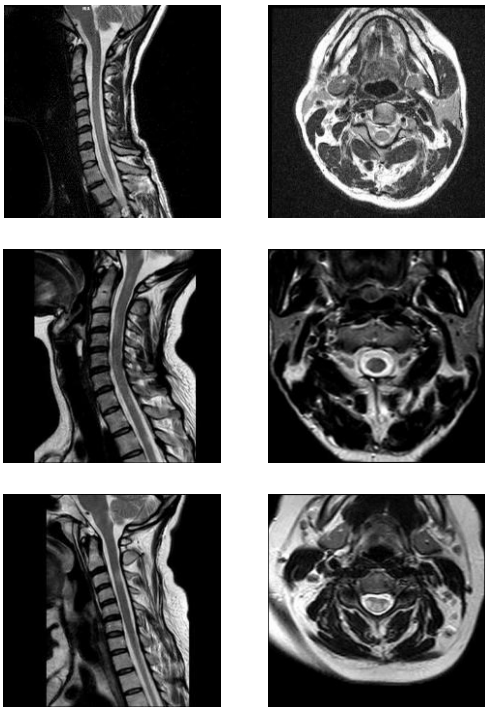

(a) (b)

Figure 2. Dataset sample images on (a) sagittal (b) axial planes

2.2. Proposed Approach

2.2.1. Feature extraction model based on FFT

Since the presence and length of lesions in MRI data vary, it is proposed that these patterns are preserved when the images are transformed into the frequency domain. Subsequently, fast Fourier transform (FFT) is applied to the MRI images. The Fourier transform captures the signal's frequency spectrum, enabling analysis and signal processing [23]. This transform provides frequency components of the signal, applied in two dimensions to the image to obtain horizontal and vertical spatial frequencies. In the resulting Fourier-transformed matrix, spectral components are concentrated based on where meaningful information is located, either at low or high frequencies [24].

In this study, frequency spectrum is extracted from MRI images using 2-D FFT. After applying 2-D FFT, a complex value matrix is obtained. The magnitude spectrum for each image is then calculated by taking the absolute value of this matrix. The different MRI data, which are shifted in the spatial domain, display different phase angles in the frequency domain [25]. By using absolute values, the spectrum remains unaffected by these shifts, effectively eliminating spatial differences in the MRI images. The steps involved in applying 2-D FFT are outlined below [26]:

Step 1. 2-D FFT application:

$$FT_{p,q} = \sum_{j=0}^{M-1}\sum_{k=0}^{N-1}\left(e^{-\frac{2\pi i}{M}}\right)^{j}\left(e^{-\frac{2\pi i}{N}}\right)^{k} X_{j+1,k+1} \quad (1)$$

Step 2. Absolute value calculation of the matrix obtained with 2D FFT:

$$MagnitudeSpectrum_{p,q} = \left|FT_{p,q}\right| \quad (2)$$

Figure 3 illustrates how the Fourier transform utilizes both the spatial arrangement and pixel values within the image.

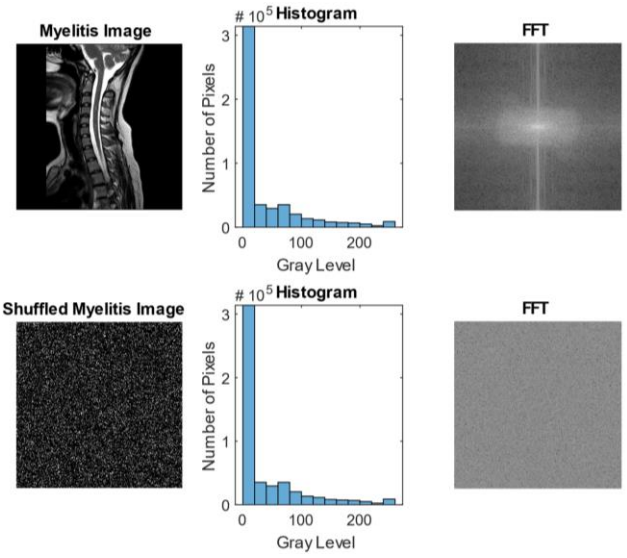

Figure 3. Histogram and FFT representation of a myelitis MRI image (first row) and the same image with pixels shuffled (second row)

Figure 3 displays an original myelitis image and the same image with shuffled pixels, their respective histograms, and the FFT results. The histograms of these images remain unchanged because the pixel values do not change. However, the FFT output differs as it utilizes spatial frequencies of pixels. This figure also illustrates the FFT's capability to extract meaningful information across pixel relationships.

2.2.1. Machine Learning with FFT

Machine learning methods rely on effective feature engineering techniques to achieve high performance, as they involve extracting underlying patterns from the data. In this study, frequency components are extracted using FFT, and their statistical features— mean value, minimum value, maximum value, standard deviation, skewness, kurtosis, and total energy— are utilized as inputs for machine learning algorithms. The equations for the skewness, kurtosis, and total energy features are provided below as (3), (4), and (5) respectively:

$$Skewness = \frac{E(x-\mu)^3}{\sigma^3} \quad (3)$$

$$Kurtosis = \frac{E(x-\mu)^4}{\sigma^4} \quad (4)$$

$$Total\ energy = \sum x^2 \quad (5)$$

In the equations, x is the vector form of the magnitude spectrum matrix. μ is the mean of x, σ is its standard deviation. E(n) is the expected value of the quantity n. The total energy magnitude is the sum of the squares of all values in the vector form of the magnitude spectrum matrix.

Support vector machine, k-nearest neighbor, and decision tree algorithms are used as machine learning classifiers. Each classifier is fed using seven normalized features extracted from the images and along with class labels for myelitis, MS or HC. As a result, the trained models are then used to predict classes for a test set that it is not previously seen. Through 10-fold cross-validation, every data point in the dataset is included in the test set at least once, ensuring robust validation of the proposed method generalization ability.

3. Experimental Results

In the study, multi-class classification is performed for HC vs. MS vs. myelitis, alongside binary class classification for HC vs. MS, MS vs. myelitis, and HC vs. myelitis. The results of these classifiers are shown using the confusion matrices, where the values in the diagonal represent the number of instances correctly classified by the respective class. The confusion matrices used in the study are illustrated in Figure 4.

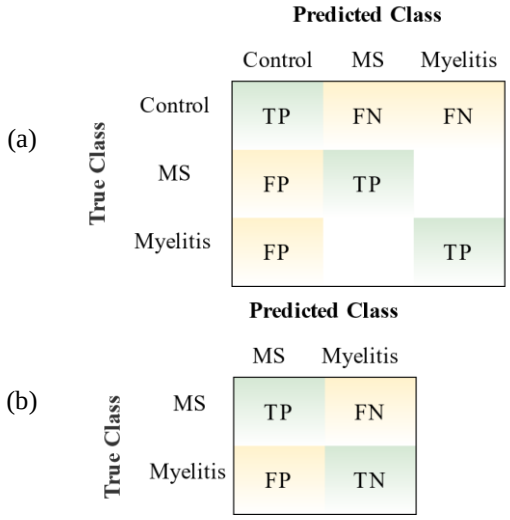

Figure 4. Confusion matrices for (a) multi-class and (b) binary class classification

Evaluation metrics are calculated with true positive (TP), false negative (FN), false positive (FP), and true negative (TP) values in the confusion matrix

3.1. Evaluation Metrics

The performance of the classifiers is evaluated by calculating accuracy, precision, recall, and F1-score values using the confusion matrix. The equations for these metrics are provided in (6) - (9) respectively:

$$Accuracy = \frac{\sum True\ Predictions}{All\ Predictions} \quad (6)$$

$$Precision = \frac{TP}{TP+FP} \quad (7)$$

$$Recall = \frac{TP}{TP+FN} \quad (8)$$

$$F1\text{-}score = \frac{2*Precision*Recall}{Precision+Recall} \quad (9)$$

When calculating the multi-class classification results, the accuracy metric is determined by the proportion of correctly predicted instances represented on the diagonal of the confusion matrix. Precision and recall metrics are computed class-wise using TP, FN, and FP values. This means that each class in the matrix is assumed to be a positive class respectively when calculating the metrics. Classifier comparisons are based on average precision and recall values.

3.2. Results for Machine Learning Models

Using FFT, frequency components are extracted and the images are re-visualized in the frequency domain. The resulting images from applying FFT to the HC, MS, and myelitis classes are shown in Figure 5.

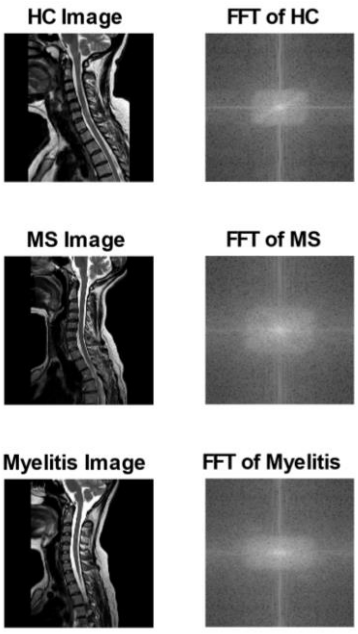

Figure 5. The example images and their FFT results in the dataset

After applying the FFT process, seven statistical features are extracted from each image. As a result, the dataset consisting of 2,746 images is transformed into a 2746x8 numerical matrix, including class labels. The training and testing phases of the classifiers are performed using 10-fold cross-validation. SVM, KNN, and decision tree classifiers are used as machine learning algorithms. By trial-and-error, the hyperparameters for SVM are set to use a cubic kernel and a box constraint level of 1. For KNN, the number of neighbors is set to 1, with the Euclidean distance metric. Lastly, the decision tree is configured with 100 splits and Gini's diversity index as the split criterion.

3.3. Multi-class Classification Results for HC, MS, and Myelitis Classes

The confusion matrices obtained by SVM, KNN, and decision tree classifiers for multi-class classification over HC, MS, and myelitis are illustrated in Figure 6.

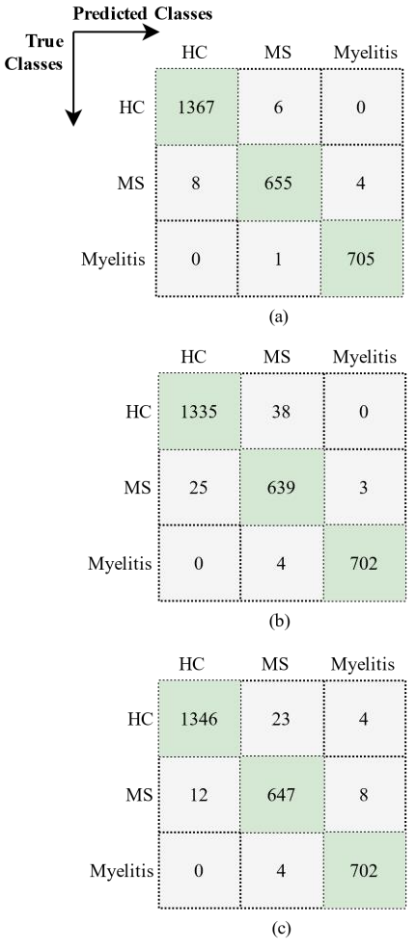

Figure 6. Confusion matrices of (a) SVM, (b) KNN, and (c) Decision Tree classifiers on multi-class classification

The diagonal values in Figure 6 indicate the number of correctly predicted instances, while outliers represent misclassified data points. Confusion matrix values indicate that the misclassification values in HC and myelitis classes are very low, and there are difficulties in distinguishing between MS and myelitis classes for all classifiers. The total misclassification costs are visualized in Figure 7.

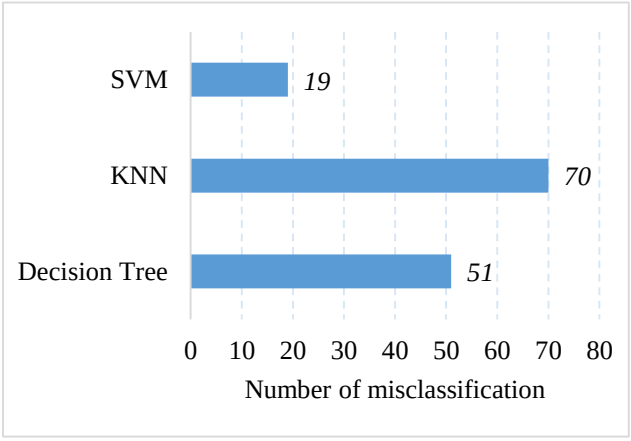

Figure 7. Total misclassification costs of the classifiers

Figure 7 shows that SVM has the lowest error with a misclassification value of 19. On the other hand, decision tree has a cost of 51, while KNN has a cost of 70.

In Table 2, the evaluation metrics calculated from the confusion matrices generated by the classifiers are presented, and precision, recall, and F1-score metrics are calculated for each class individually. Additionally, average precision, recall, and F1-score values are provided to compare the overall performance of the classifiers. Accuracy is presented as a single value, calculated based on the classifiers' correct predictions of the class labels.

Overall, the SVM classifier achieves the highest classification rate with 99.31% accuracy, along with an average precision of 99.27%, average recall of 99.21%, and average F1-score of 99.24%. The KNN classifier achieves 97.45% accuracy, with average precision, recall, and F1-score values of 97.19%, 97.49%, and 97.34% respectively. The decision tree obtains an accuracy of 98.14%, along with average precision, recall, and F1-score values of 97.81%, 98.16%, and 97.98% respectively.

Table 2. Multi-class classification evaluation results

Classifiers	Classes	Evaluation metrics (%)			
		Precision	Recall	F1-score	Accuracy
SVM	Healthy Control	99.42	99.56	99.49	99.31
	MS	98.94	98.20	98.57	
	Myelitis	99.44	99.86	99.65	
	Average values	*99.27*	*99.21*	*99.24*	
KNN	Healthy Control	98.16	97.23	97.69	97.45
	MS	93.83	95.80	94.81	
	Myelitis	99.57	99.43	99.50	
	Average values	*97.19*	*97.49*	*97.34*	
Decision Tree	Healthy Control	99.12	98.03	98.57	98.14
	MS	95.99	97.00	96.50	
	Myelitis	98.32	99.43	98.87	
	Average values	*97.81*	*98.16*	*97.98*	

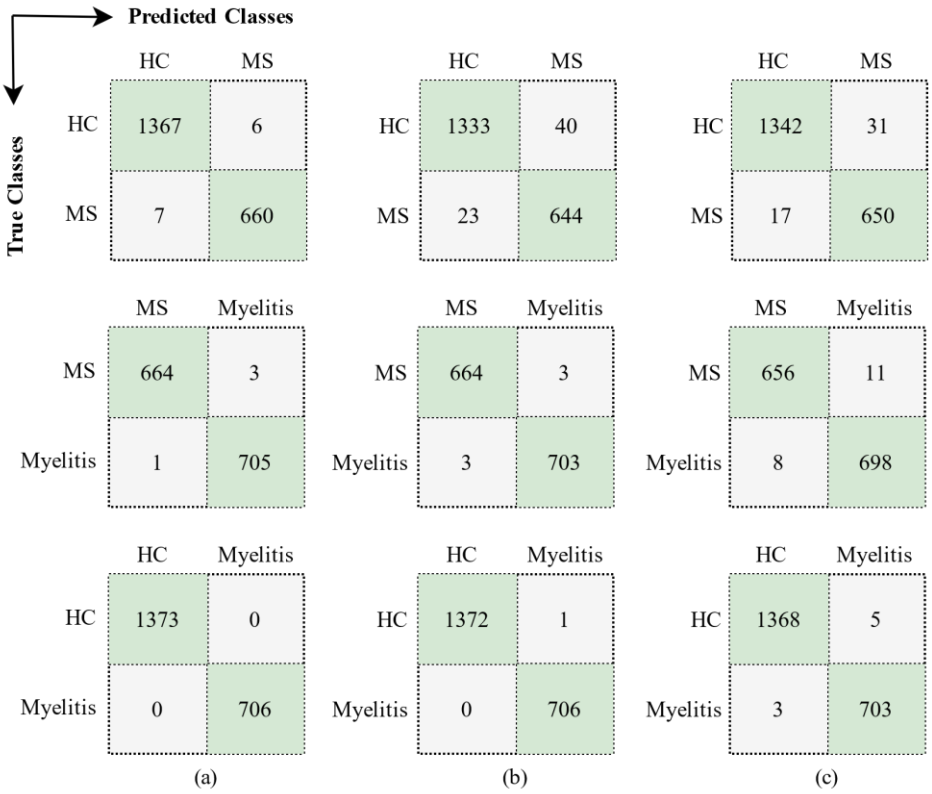

Figure 8. Confusion matrices of (a) SVM, (b) KNN, and (c) Decision Tree classifiers on binary class classification

3.4. Binary Class Classification Results

In addition to multiclass classification, the performance of the FFT method on binary classification is evaluated. This analysis involves using the feature set created in the study to classify between two classes. Binary class classification is performed for HC vs. MS, MS vs. myelitis, and HC vs. myelitis. The confusion matrices generated by SVM, KNN, and decision tree classifiers are shown in Figure 8.

According to Figure 8, among 2,040 images, SVM has 13 misclassification cost, the KNN has a cost of 63, and the decision tree has a cost of 48 for HC vs. MS classification. Among 1,343 images for MS vs. myelitis classification, SVM has 4 misclassification cost, the KNN has a cost of 6, and the decision tree is a cost of 19. Among 2,079 images for HC vs. myelitis classification, SVM has zero misclassification cost, the KNN has a cost of 1, and the decision tree is a cost of 8. Visual representations of misclassification costs are illustrated in Figure 9.

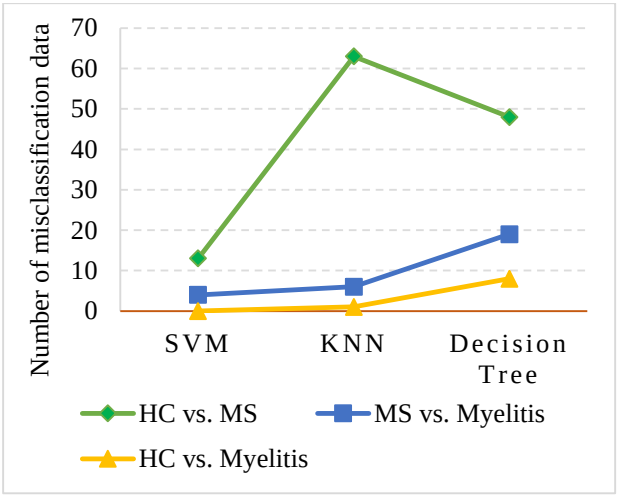

Figure 9. Confusion matrices of (a) SVM, (b) KNN, and (c) Decision Tree classifiers on binary class classification

The calculated evaluation metrics are detailed in Table 3. The results demonstrate that SVM achieves the highest accuracy values across all binary classifications. It gets an accuracy of 99.36% for HC vs. MS, 99.71% for HC vs. MS, and 100% for HC vs. MS. KNN also shows successful evaluation metrics, performing better than the decision tree in all categories except HC vs. MS classification. These results indicate that FFT combined with statistical features exhibits superior performance as a feature extraction method, resulting in minimal misclassification costs, particularly with the SVM classifier. Notably, SVM achieves perfect predictions for HC vs. myelitis classes. The general results obtained can be summarized as follows: (1) Proposed FFT+statistical features model achieves the highest successful results on HC and myelitis classes, (2) the highest misclassification cost is observed between HC and MS classes, (3) SVM displays the highest evaluation metric results, (4) the decision tree outperforms KNN in predicting HC and MS classes.

4. Discussion

4.1. Analysis of the proposed approach's performance results

The dataset for myelitis, MS, and healthy control classes, consisting of axial and sagittal MRI images, is re-visualized in the frequency domain using FFT. Subsequently, seven statistical features—mean value, minimum and maximum values, skewness, kurtosis, and total energy—are extracted from the frequency spectrum.

Multi-class classification and binary class classification are performed and the results are analyzed separately. According to the results obtained by SVM, KNN, and decision tree classifiers, it is observed that the MRI data in the frequency domain with FFT preserved the distinctive features of the classes. Among the classifiers, the SVM achieves the highest accuracy. While calculating the evaluation metrics, each class is selected as a positive class in turn, and class-wise metrics are averaged to analyze the method's success. In the classification of the three classes, the SVM algorithm correctly classified 2,727 data out of 2,746 images, misclassifying 19 images. As a result, SVM achieves 99.31% accuracy, 99.27% precision, 99.21% recall, and a 99.24% F1-score. The decision tree performs better than KNN, with an accuracy of 98.14%. When analyzed on the class-wise basis, the decision tree is particularly successful in classifying healthy control and MS classes, while KNN shows higher success in myelitis classification. Another outcome of the study is the relatively lower classification success in the MS class. Nevertheless, the feature set generated by the proposed method enables SVM and KNN to effectively discriminate healthy control and myelitis classes, achieving a satisfactory success rate.

When the FFT method is applied to MRI data, low-frequency components are located in the center of the spectrum, providing information about the overall structure of the image. High-frequency components, which spread out to the edges, represent distinctive details, thereby analyzing intensity variations between pixels.

Table 3. Binary class classification evaluation results

Classifiers	Classes	Evaluation metrics (%)			
		Precision (average)	Recall (average)	F1-score (average)	Accuracy
SVM	HC vs. MS	99.29	99.26	99.28	99.36
	MS vs. myelitis	99.71	99.70	99.71	99.71
	HC vs. myelitis	100	100	100	100
KNN	HC vs. MS	96.23	96.82	96.51	96.91
	MS vs. myelitis	99.56	99.56	99.56	99.56
	HC vs. myelitis	99.93	99.96	99.95	99.95
Decision Tree	HC vs. MS	97.10	97.60	97.34	97.65
	MS vs. myelitis	98.62	98.61	98.61	98.62
	HC vs. myelitis	99.54	99.61	99.57	99.62

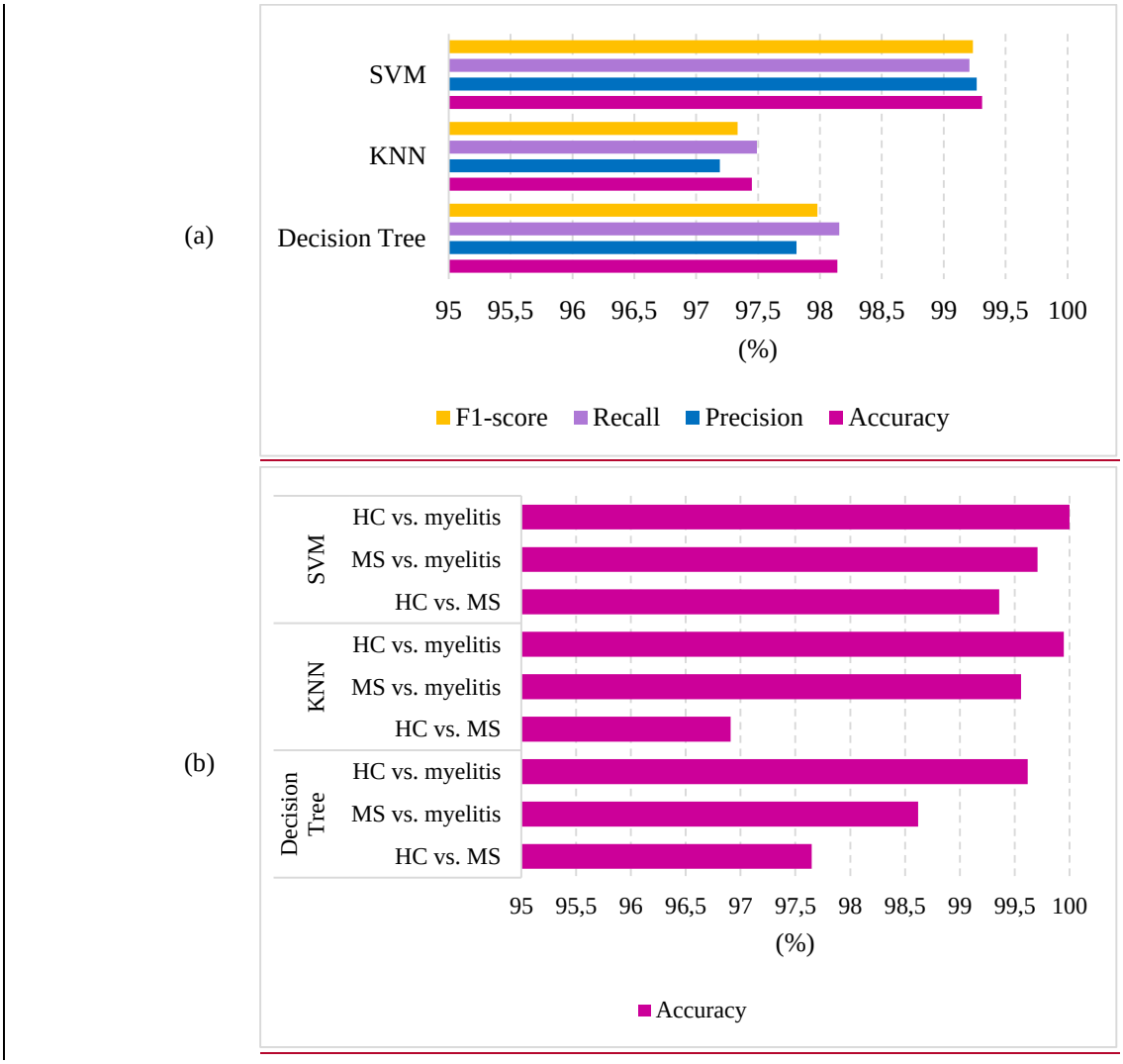

Figure 10. Visual comparison of evaluation metrics for (a) multi-class (b) binary class classification

The results of both multi-class and binary class classification show high accuracies for the healthy control and myelitis classes, with relatively lower accuracies for MS. This is likely due to the vertebral length of the lesions in the spinal cord; more extensive lesions cause stronger pixel intensity changes, making the easier for the FFT to distinguish. An analysis of the binary class classification results reveals that the most confusion for the classifiers occurs between healthy control and MS classes. In contrast, SVM and KNN almost perfectly detects healthy control and myelitis classes, achieving 100%

and 99.95% accuracy, respectively. These results imply that the FFT combined with statistical features effectively extracts image patterns and preserves the distinguishing features between classes. As a result, balanced evaluation metrics are achieved without any class dominance. Figure 10 shows summarized visualizations of performance metrics for multi-class and binary class classification.

Figure 10(a) illustrates for multi-class classification that the proposed FFT+statistical features model shows the highest success with SVM for HC vs. myelitis. The classifiers achieve lower classification success for HC vs. MS among all binary class classification. The proposed method achieves over 96.5% classification success in all classifiers for all binary classes. Figure 10(b) illustrates for binary classification that SVM achieves over 99% success in all metrics. Decision tree obtains better results than KNN, and all classifiers gets balanced/proportional success in all metrics.

4.2. Comparative analysis with other studies and alternative dataset

In order to detect myelitis, MS, and healthy control, the performance of the FFT+statistical features method proposed in this study is compared with another study [20], which utilizes on the same dataset (Myelitis Dataset).

Additionally, the proposed FFT+statistical features model is applied to another dataset from Kaggle [27], containing MRI data of MS and healthy control classes. This dataset comprises both axial and sagittal images, totaling 3,427 images, including 1,411 MS images and 2,016 healthy control images (MS Dataset). All the steps applied to the Myelitis dataset are also applied to this MS dataset, and the results obtained by SVM are listed in Table 4.

Table 4. Overall performance comparison with other studies

Datasets	Method	Evaluation metrics			
		Accuracy	Precision	Recall	F1-score
Myelitis Dataset	Tatli et al. [20]	97.63	97.23	97.23	97.23
(HC vs. MS vs. myelitis)	The proposed model	99.31	99.27	99.21	99.24
MS Dataset	Macin et al. [27]	98.22	99.27	96.39	97.81
(HC vs. MS)	Ekmekyapar and Taşcı [28]	98.02	98.31	97.63	97.94
	The proposed model	99.91	99.93	99.89	99.91

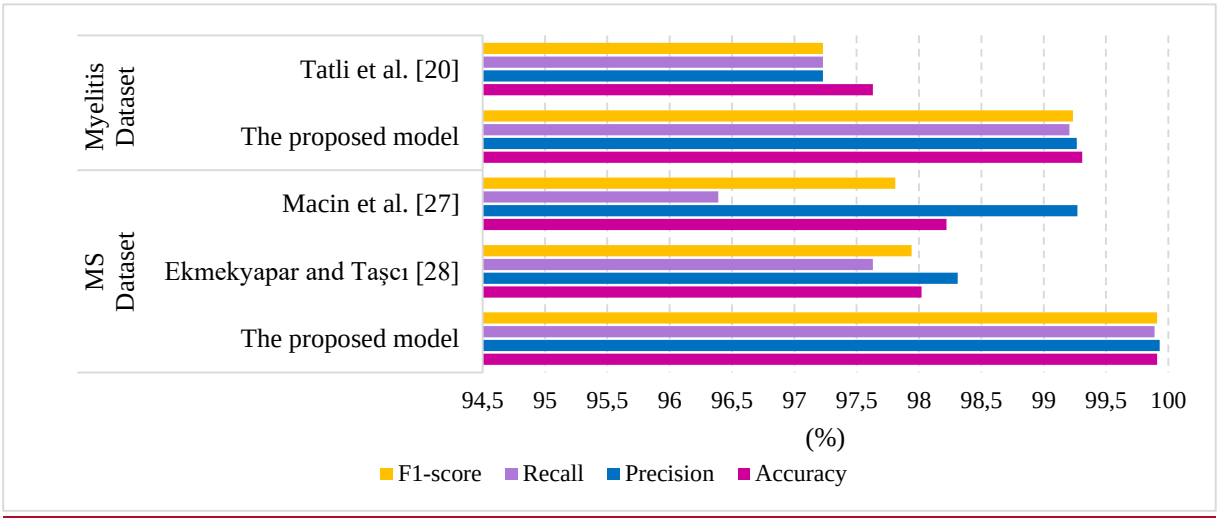

Figure 11. Evaluation metrics comparisons with other studies and datasets

According to Table 4, the method proposed in this paper achieves higher success in all metrics across both datasets. As shown in Figure 11, the bar graph illustrates that the proposed method in this study outperforms the other studies on all evaluated metrics.

5. Conclusion

In this study, it is proposed that visualizing myelitis, MS, and HC MRI images in the frequency domain using FFT is preserve important patterns in statistical features of these images, aiding in class detection. The effectiveness of the proposed feature extraction method is tested using classifiers. SVM, KNN, and decision tree, which are commonly used machine learning algorithms in biomedical image classification, are employed to detect myelitis, MS, and healthy control classes. According to the results, SVM achieves 99.31% correct classification accuracy for multiclass classification after applying the FFT method to MRI images. The method's average precision (99.27%), recall (99.21%), and F1-score (99.24%) values indicate balanced classification across all classes. Additionally, for binary class classification, the proposed FFT+statistical features combination demonstrates superior performance with the SVM classifier, achieving 99.36% accuracy (HC vs. MS), 99.71% accuracy (MS vs. myelitis), 100% accuracy (HC vs. myelitis). These results show that the statistical features of the FFT-transformed images effectively formed patterns that characterize the classes, confirming their utility as a highly successful feature extractor. As a future work, the FFT method can be applied to different biomedical data sets, or its performance can be analyzed by combining it with deep learning models.

References

[1] E. Glucksman, C. Medina, J. Phillips, R. Schlussel, and S. Glucksman, "New onset urinary incontinence in a pediatric patient with transverse myelitis," *Urol Case Rep*, vol. 46, p. 102322, January 2023.

[2] Y. S. Abuzneid, H. Al-Janazreh, M. Haif, S. T. Idais, B. Asakrah, S. M. Ajwa, et al., "Radiation induced delayed transverse myelitis and neurological deficit at tertiary care center," *Ann Med Surg (Lond)*, vol. 69, p. 102728, September 2021.

[3] S. Lopez Chiriboga and E. P. Flanagan, "Myelitis and Other Autoimmune Myelopathies," *Continuum (Minneap Minn)*, vol. 27, pp. 62-92, February 2021.

[4] S. Presas-Rodríguez, L. Grau-López, J. V. Hervás-García, A. Massuet-Vilamajó, and C. Ramo-Tello, "Myelitis: Differences between multiple sclerosis and other aetiologies," *Neurología (English Edition)*, vol. 31, 2016, pp. 71-75.

[5] Z. Yılmaz Acar, F. Başçiftçi, and A. H. Ekmekci, "Future activity prediction of multiple sclerosis with 3D MRI using 3D discrete wavelet transform," *Biomedical Signal Processing and Control*, vol. 78, p. 103940, September 2022.

[6] M. K. Yagnavajjula, K. R. Mittapalle, P. Alku, S. R. K, and P. Mitra, "Automatic classification of neurological voice disorders using wavelet scattering features," *Speech Communication*, vol. 157, p. 103040, February 2024.

[7] K. Hackmack, F. Paul, M. Weygandt, C. Allefeld, and J.-D. Haynes, "Multi-scale classification of disease using structural MRI and wavelet transform," *NeuroImage*, vol. 62, pp. 48-58, August 2012.

[8] J. Feng, S.-W. Zhang, and L. Chen, "Identification of Alzheimer's disease based on wavelet transformation energy feature of the structural MRI image and NN classifier," *Artificial Intelligence in Medicine*, vol. 108, p. 101940, August 2020.

[9] Z. Ding, Y. Liu, X. Tian, W. Lu, Z. Wang, X. Zeng, et al., "Multi-resolution 3D-HOG feature learning method for Alzheimer's Disease diagnosis," *Computer Methods and Programs in Biomedicine*, vol. 214, p. 106574, February 2022.

[10] E. Kaplan, M. Baygin, P. D. Barua, S. Dogan, T. Tuncer, E. Altunisik, et al., "ExHiF: Alzheimer's disease detection using exemplar histogram-based features with CT and MR images," *Medical Engineering & Physics*, vol. 115, p. 103971, May 2023.

[11] S. Abbasi and F. Tajeripour, "Detection of brain tumor in 3D MRI images using local binary patterns and histogram orientation gradient," *Neurocomputing*, vol. 219, pp. 526-535, January 2017.

[12] Z. Yılmaz Acar, F. Başçiftçi, and A. H. Ekmekci, "A Convolutional Neural Network model for identifying Multiple Sclerosis on brain FLAIR MRI," *Sustainable Computing: Informatics and Systems*, vol. 35, p. 100706, September 2022.

[13] P. Varalakshmi, B. Tharani Priya, B. Anu Rithiga, R. Bhuvaneaswari, and R. Sakthi Jaya Sundar, "Diagnosis of Parkinson's disease from hand drawing utilizing hybrid models," *Parkinsonism & Related Disorders*, vol. 105, pp. 24-31, December 2022.

[14] I. K. Veetil, D. E. Chowdary, P. N. Chowdary, V. Sowmya, and E. A. Gopalakrishnan, "An analysis of data leakage and generalizability in MRI based classification of Parkinson's Disease using explainable 2D Convolutional Neural Networks," *Digital Signal Processing*, vol. 147, p. 104407, April 2024.

[15] S. E. Sorour, A. A. A. El-Mageed, K. M. Albarrak, A. K. Alnaim, A. A. Wafa, and E. El-Shafeiy, "Classification of Alzheimer's disease using MRI data based on Deep Learning Techniques," *Journal of King Saud University - Computer and Information Sciences*, vol. 36, p. 101940, February 2024.

[16] M. Menagadevi, S. Devaraj, N. Madian, and D. Thiyagarajan, "Machine and deep learning approaches for alzheimer disease detection using magnetic resonance images: An updated review," *Measurement*, vol. 226, p. 114100, February 2024.

[17] A. Basher, B. C. Kim, K. H. Lee, and H. Y. Jung, "Volumetric Feature-Based Alzheimer's Disease Diagnosis From sMRI Data Using a Convolutional Neural Network and a Deep Neural Network," *IEEE Access*, vol. 9, pp. 29870-29882, 2021.

[18] A. Ebrahimi, S. Luo, and A. s. D. Neuroimaging Initiative, "Convolutional neural networks for Alzheimer's disease detection on MRI images," *Journal of Medical Imaging*, vol. 8, p. 024503, 2021.

[19] D. Venkatesan, A. Elangovan, H. Winster, M. Y. Pasha, K. S. Abraham, S. J, et al., "Diagnostic and therapeutic approach of artificial intelligence in neuro-oncological diseases," *Biosensors and Bioelectronics: X*, vol. 11, p. 100188, September 2022.

[20] S. Tatli, G. Macin, I. Tasci, B. Tasci, P. D. Barua, M. Baygin, et al., "Transfer-transfer model with MSNet: An automated accurate multiple sclerosis and myelitis detection system," *Expert Systems with Applications*, vol. 236, p. 121314, February 2024.

[21] J. Kunhoth, S. Al Maadeed, M. Saleh, and Y. Akbari, "CNN feature and classifier fusion on novel transformed image dataset for dysgraphia diagnosis in children," *Expert Systems with Applications*, vol. 231, p. 120740, November 2023.

[22] F. Hassan, S. F. Hussain, and S. M. Qaisar, "Fusion of multivariate EEG signals for schizophrenia detection using CNN and machine learning techniques," *Information Fusion*, vol. 92, pp. 466-478, April 2023.

[23] Q. Gao, A. H. Omran, Y. Baghersad, O. Mohammadi, M. A. Alkhafaji, A. K. J. Al-Azzawi, et al., "Electroencephalogram signal classification based on Fourier transform and Pattern Recognition Network for epilepsy diagnosis," *Engineering Applications of Artificial Intelligence*, vol. 123, p. 106479, August 2023.

[24] M. S. Nixon and A. S. Aguado, "Chapter 2 - Images, sampling, and frequency domain processing," in Feature Extraction & Image Processing for Computer Vision (Third Edition), M. S. Nixon and A. S. Aguado, Eds., ed Oxford: Academic Press, 2012, pp. 37-82.

[25] P. Han, *Feature extraction and descriptor based on Fourier transform of local images*, Master Thesis, Department of Computer Science, The University of Regina (Canada), 2022.

[26] M. Li and W. Chen, "FFT-based deep feature learning method for EEG classification," *Biomedical Signal Processing and Control*, vol. 66, p. 102492, April 2021.

[27] G. Macin, B. Tasci, I. Tasci, O. Faust, P. D. Barua, S. Dogan, et al., "An Accurate Multiple Sclerosis Detection Model Based on Exemplar Multiple Parameters Local Phase Quantization: ExMPLPQ," *Applied Sciences*, vol. 12, p. 4920, 2022.

[28] T. Ekmekyapar and B. Taşcı, "Exemplar MobileNetV2-Based Artificial Intelligence for Robust and Accurate Diagnosis of Multiple Sclerosis," *Diagnostics*, vol. 13, p. 3030, 2023.